Aalborg Universitet

A Spatial Decision Support Approach for Flood Vulnerability Analysis in Urban Areas

A Case Study of Tehran

Afsari, Rasoul; Shorabeh, Saman Nadizadeh; Kouhnavard, Mostafa; Homaee, Mehdi; Arsanjani, Jamal Jokar

Article

A Spatial Decision Support Approach for Flood Vulnerability Analysis in Urban Areas: A Case Study of Tehran

Rasoul Afsari [1], Saman Nadizadeh Shorabeh [2], Mostafa Kouhnavard [3], Mehdi Homaee [4,†]
and Jamal Jokar Arsanjani [5,*]

[1] School of Architecture & Environmental Design, Iran University of Science & Technology, Tehran 1684613114, Iran; afsari_r@arch.iust.ac.ir
[2] Department of GIS and Remote Sensing, Faculty of Geography, University of Tehran, Tehran 1417853933, Iran; saman.nadizadeh@ut.ac.ir
[3] Department of Urban Planning, Faculty of Social Sciences, Allameh Tabataba'i University, Tehran 1544915113, Iran; Mostafa.koohnavard7667@gmail.com
[4] Department of Mining and Environmental Engineering, Faculty of Engineering, Tarbiat Modares University, Tehran 14115, Iran; mhomaee@modares.ac.ir
[5] Department of Planning, Geoinformatics and Earth Observation Research Group, Aalborg University Copenhagen, 2450 Copenhagen, Denmark
[*] Correspondence: jja@plan.aau.dk
[†] Agrohydrology Research Group (Grant Number. IG-39713), Tarbiat Modares University, Tehran 14115, Iran.

Abstract: Preparedness against floods in a hazard management perspective plays a major role in the pre-event phase. Hence, assessing urban vulnerability and resilience towards floods for different risk scenarios is a prerequisite for urban planners and decision makers. Therefore, the main objective of this study is to propose the design and implementation of a spatial decision support tool for mapping flood vulnerability in the metropolis of Tehran under different risk scenarios. Several factors reflecting topographical and hydrological characteristics, demographics, vegetation, land use, and urban features were considered, and their weights were determined using expert opinions and the fuzzy analytic hierarchy process (FAHP) method. Thereafter, a vulnerability map for different risk scenarios was prepared using the ordered weighted averaging (OWA) method. Based on our findings from the vulnerability analysis of the case study, it was concluded that in the optimistic scenario (ORness = 1), more than 36% of Tehran's metropolis area was marked with very high vulnerability, and in the pessimistic scenario (ORness = 0), it was less than 1% was marked with very high vulnerability. The sensitivity analysis of our results confirmed that the validity of the model's outcomes in different scenarios, i.e., high reliability of the model's outcomes. The methodical approach, choice of data, and the presented results and discussions can be exploited by a wide range of stakeholders, e.g., urban planners, decision makers, and hydrologists, to better plan and build resilience against floods.

Keywords: vulnerability mapping; GIS; risk in decision making; sensitivity analysis; Tehran

1. Introduction

Rapid urbanization and the lack of sufficient infrastructure alongside climate change have presented unprecedented environmental hazards jeopardizing societal security [1,2]. In the meantime, floods are considered as the most serious natural hazards worldwide [3,4] because they cause human losses and adverse effects on social and environmental development [5,6], as well as financial losses, which are equivalent to 40% of the total economic losses caused by natural hazards per year [7]. Global warming [8], low soil infiltration and storage capacity during storm events [9], poor drainage system [10], population growth and spatial expansion, and the consequent heterogeneous urban growth [11] are the main causes of floods in urban areas. Between 1998 and 2015, floods alone affected 2.3 billion

people worldwide [12], 95% of which live in Asia. According to Luo et al. [13], around 21 million people worldwide are affected by river floods each year, which may increase to 54 million by 2030 due to socio-economic growth and climate change [8]. Therefore, assessing urban flood vulnerability and disseminating this information to all stakeholders in urban flood management is very important. Vulnerability is a condition that is determined by physical, socio-economic and environmental factors or processes and reduces the preparedness of communities for the effects and consequences of hazards [14]. Vulnerability is highly dependent on environmental conditions and contexts. In many cases, similar outcomes are different in different social and economic situations, and these differences can be attributed to the spatial distinction of vulnerability [15].

Due to its massive areal coverage, geographical location, topographic characteristics, and climatic diversity, Iran is among the countries that are exposed to high damage from natural hazards. For instance, out of 41 known accidents in the world, 31 to 33 types have a history in Iran, the most common of which is floods [16]. Meanwhile, the metropolis of Tehran, with an area of about 730 km², is one of the largest cities in the world, with special features and specifications. Tehran has 22 urban regions and a high concentration of government organizations, industries, facilities, and services, which make its management very complicated in the event of a natural hazard. Tehran has the highest positive incoming migration rate since 1976. The main part of this event was due to socio-economic opportunities and inequality in terms of services and wealth distribution [17]. This wave of migration has led to an unprecedented boom in the construction industry, turning open lands and grasslands into impervious surfaces. Several factors have contributed to witnessing large number of floods in Tehran, such as physical development ranging from 700 m to 2200 m of elevation; steep slopes in the northern and eastern parts of the city on the doorstep of the Alborz mountains; extensive urban and industrial development, even in the riverbeds; ignoring the ecosystem services; reduced soil infiltration; and the lack of an efficient and proper sewage network. Therefore, mapping vulnerable areas of Tehran against floods in order to minimize its consequences is crucial for a better allocation of resources.

The general purpose of multi-criteria decision analysis (MCDA) is to assist in the process of decision making by facilitating the selection of the most optimal choice among existing options. These techniques operate on a combination of spatial data and user preferences, according to a predefined decision rule [18–20]. The underlying logic behind integrating the geographical information system (GIS) and MCDA is that these two separate fields of study may act in synergy with one another [21,22]. On the one hand, GIS-technology provides a comprehensive tool for storing, manipulating, analysing, and representing geographical information, while MCDA yields a rich array of structural methods and algorithms for decision making, design, evaluation, and prioritization of options. The idea behind this integration is to extend GIS-based technology to give the user (decision maker) a degree of control over preferences (priorities of options) [23,24]. The main relevance of MCDA to spatial decision making is its capacity for identifying the most optimal solution and constructing a structured and creative approach to problem solving [25,26].

In the field of flood vulnerability modelling, various studies have been performed using MCDA methods and GIS [27–31]. For example, Chakraborty and Mukhopadhyay [32] investigated urban flood vulnerability in Bengal, India, using GIS–Analytic Hierarchy Process (AHP). They used spatial criteria in two categories of vulnerability and risk. In addition, the AHP method was used to obtain the weight of the criteria, and the linear weight combination method was used to combine the criteria. Their results showed that vulnerability levels are higher at areas located particularly along the India–Bangladesh international border in the south, southeast, and southwest and in some isolated clusters in the central and north-central parts. Eini et al. [33] evaluated flood vulnerability in Kermanshah. This study employed the fuzzy analytic hierarchy process (FAHP) method. Economic, social, and infrastructural criteria were considered for flood vulnerability analysis. The results indicated that the infrastructure criterion has the highest impact weight on the

vulnerability. In general, population, urban texture, and distance to the major drainage channels are the most important factors in increasing flood risk. Similarly, Feloni et al. [34] identified flood-prone areas in Attica, Greece, using the FAHP method. Morphological and hydrological criteria were used. They concluded that, regarding the Attica region, the potentially flood-prone areas are concentrated in the Attica basin and in the lowlands of Western and Eastern Attica. Hadipour et al. [35] used the AHP–Weighted Linear Combination (WLC) combination to map flood vulnerability in Bandar Abbas. They used a total of 10 spatial criteria. A total of 10 spatial criteria were considered. They used the AHP-WLC combination to gain weight and prepare for flood vulnerability. A total of 10 spatial criteria were considered. They used the AHP-WLC combination to gain weight and prepare for flood vulnerability. The vulnerability map showed that the eastern and western regions have a larger area of very high vulnerability class. In a study in Melbourne, Rashetnia and Jahanbani [36] developed a fuzzy-rule-based flood vulnerability index considering the hydrological, social, and economic aspects of flood damages to assess and map flood vulnerability. It was found that 51.6% of the total area of the study area was in the class with low and very low vulnerability, while 7.6% was in the class with high and very high vulnerability. Hussain et al. [37] used the GIS-WLC technique to identify flood-vulnerable areas in Khyber Pakhtunkhwa, Pakistan. A set of 18 criteria was divided into three categories: physical, socioeconomic, and coping capacity. The results demonstrated that 25% of the western-middle area to the northern part of the study area comprises high to very high vulnerability because of the proximity to waterways, high rainfall, elevation, and other socioeconomic factors.

A review of previous studies shows that in order to prepare a flood vulnerability map, first, the effective criteria were identified, and then a classified vulnerability map was created using a combination of different criteria. However, none of the models used in previous studies has included the concept of risk in the decision to map flood vulnerability. Therefore, this study attempts to address this important research gap for the first time. The ordered weighted averaging (OWA) model is used to inject the concept of risk in decision making and vulnerability mapping in multiple scenarios, the results of which can facilitate the decision-making process for managers and planners.

The paper is organized as follows: Section 2 provides a brief description of the study area and describes the materials and methods used; Section 3 reports the results of the analysis; Section 4 discusses the implication of the results; and Section 5 discusses the conclusions that can be drawn.

2. Materials and Methods

2.1. Study Area and Data

Tehran city is the centre of Tehran province and is the most populous city and the capital of Iran. With a population of 9,259,009, it is the 37th most populous city in the world. The city is geographically located at 51°17′ to 51°33′ E and 35°36′ to 35°45′ N (Figure 1). Tehran is spread on the southern slopes of the Alborz Mountain range. Annual rainfall in Tehran is intentionally affected by altitude differences. It is 422 mm in the north and 145 mm in the south. The number of rainy days follows this pattern, which varies between 89 days in the north and 33 days in the south [38]. Numerous rivers drain rainwater and transfer it to the plains downstream. The general direction of rivers and canals is mainly towards the urban area. This can cause flash floods in the streets of Tehran, and if the storms are heavy and the rain continues, floods will occur. At the same time, the urban area of Tehran hosts several canals and rivers that are responsible for the drainage of the upstream basins as well as the collection of rainwater in the urban area of Tehran. In some parts of the city, where the price of land is high, the bed of rivers and water channels inside the city have been attacked, and their cross-section has been reduced and limited. This can affect the natural regime of the river and the flow path and cause irreparable damage in the event of heavy rainfalls.
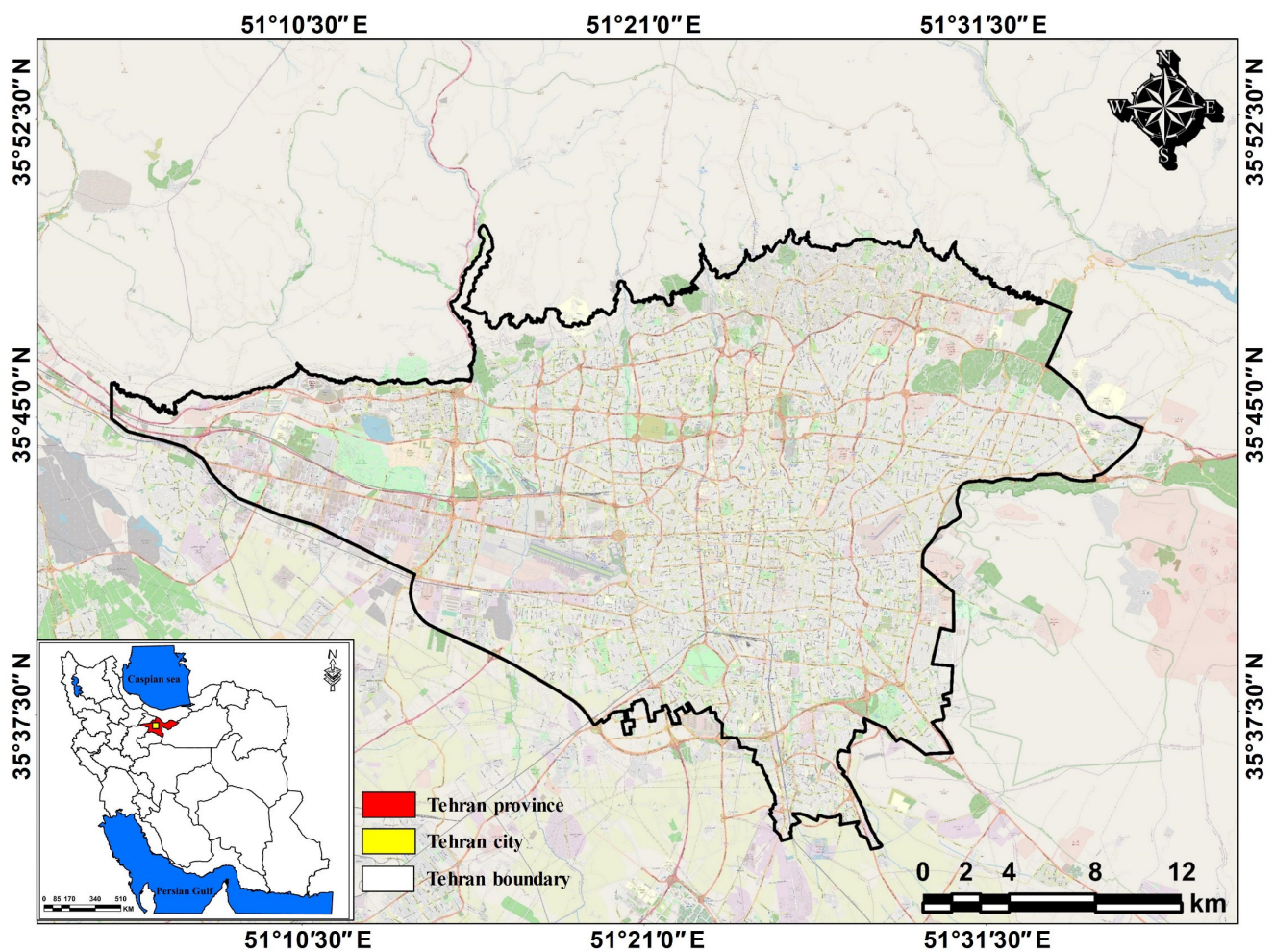
Figure 1. Geographical location of the study area.

In general, the surface water of the Tehran Basin consists of three systems: (i) rivers and streams (such as the Kan river) that flow to the southwest of Tehran; (ii) rivers and streams (such as the Sorkheh Hesar river) that flow southeast of Tehran; and (iii) streams and canals (such as the Darband river) in the central and southern parts of Tehran [39]. Sudden flood events reported in Tehran are shown in Table 1. The first recorded flood was in 1954, in which 2154 people died. In 1987, heavy rains caused flooding of surface waters, injuring 1027 people and killing 1010. It also caused more than USD 7 million in economic losses. In total, 1267 people have been injured and 3482 have died in floods since 1954.

Table 1. Summary of the floods that occurred in Tehran (Adapted with permission from [17]).

Year	Death	Injured-Missing People	Houses Destroyed and Damaged	Economic Losses (K$)
1954	2150	-	-	-
1955–1986	118	40	-	10,700
1987	1010	1027	862	7,655,000
1988	146	106	100	150,000
1989–2010	39	65	348	38,000
2012	8	7	-	21,000
2015	11	22	-	-

In this study, raster and vector spatial datasets were used to prepare a flood vulnerability map. Raster data included elevation, slope, aspect, vegetation density, rainfall, land use, flow accumulation, and impervious surfaces. Vector data included population density, river, health centres, road, soil type, and fire station. Expert knowledge was used to obtain the weight of criteria, ArcGIS was used for pre-processing of the layers and spatial analysis, and IDRISI was used to prepare a vulnerability map. The research data specifications are shown in Table 2.

Table 2. Characteristics of the used data.

Row	Data	Resolution/Scale	Source
1	elevation	30 m	https://earthexplorer.usgs.gov/ (accessed on 12 February 2021)
2	slope	30 m	Extracted from the Digital Elevation Model (DEM)
3	aspect	30 m	Extracted from the DEM
4	population density	1:2000	https://www.tehran.ir/ (accessed on 8 April 2021)
5	river	1:50,000	https://frw.ir/ (accessed on 25 January 2021)
6	vegetation density	30 m	https://earthexplorer.usgs.gov/ (accessed on 18 April 2022)
7	land use	30 m	https://earthexplorer.usgs.gov/ (accessed on 22 February 2021)
8	flow accumulation	30 m	Extract from the DEM
9	impervious surfaces	30 m	https://earthexplorer.usgs.gov/ (accessed on 22 February 2021)
10	fire stations	1:50,000	https://www.tehran.ir/ (accessed on 8 April 2021)
11	health centres	1:50,000	https://www.tehran.ir/ (accessed on 8 April 2021)
12	soil type	1:100,000	https://gsi.ir/ (accessed on 25 January 2021)
13	rainfall	250 m	https://wapor.apps.fao.org/ (accessed on 25 January 2021)
14	road	1:50,000	http://www.ncc.org.ir/ (accessed on 18 March 2021)

2.2. Methodology

Six main steps were taken in this study to prepare a vulnerability map of urban areas to floods (Figure 2):

Step 1: Using expert opinions and the research literature, important and effective criteria were identified to determine the vulnerability of urban areas to floods. After collecting the criteria based on a pairwise scale model, a questionnaire on criteria weighting was presented to experts.

Step 2: Using a set of GIS spatial analysis tools for these criteria, the information layers were prepared as GIS maps. GIS layers were then assigned to these criteria.

Step 3: Using the expert opinions and the weighting method of FAHP, the weight of each layer and criterion was calculated.

Step 4: Minimum and maximum functions were used for dimensionless criterion mapping.

Step 5: By combining the criteria map using the OWA model, a map of urban area vulnerability to floods in different degrees of risk was prepared.

Step 6: The modelling results were evaluated using the sensitivity analysis method.
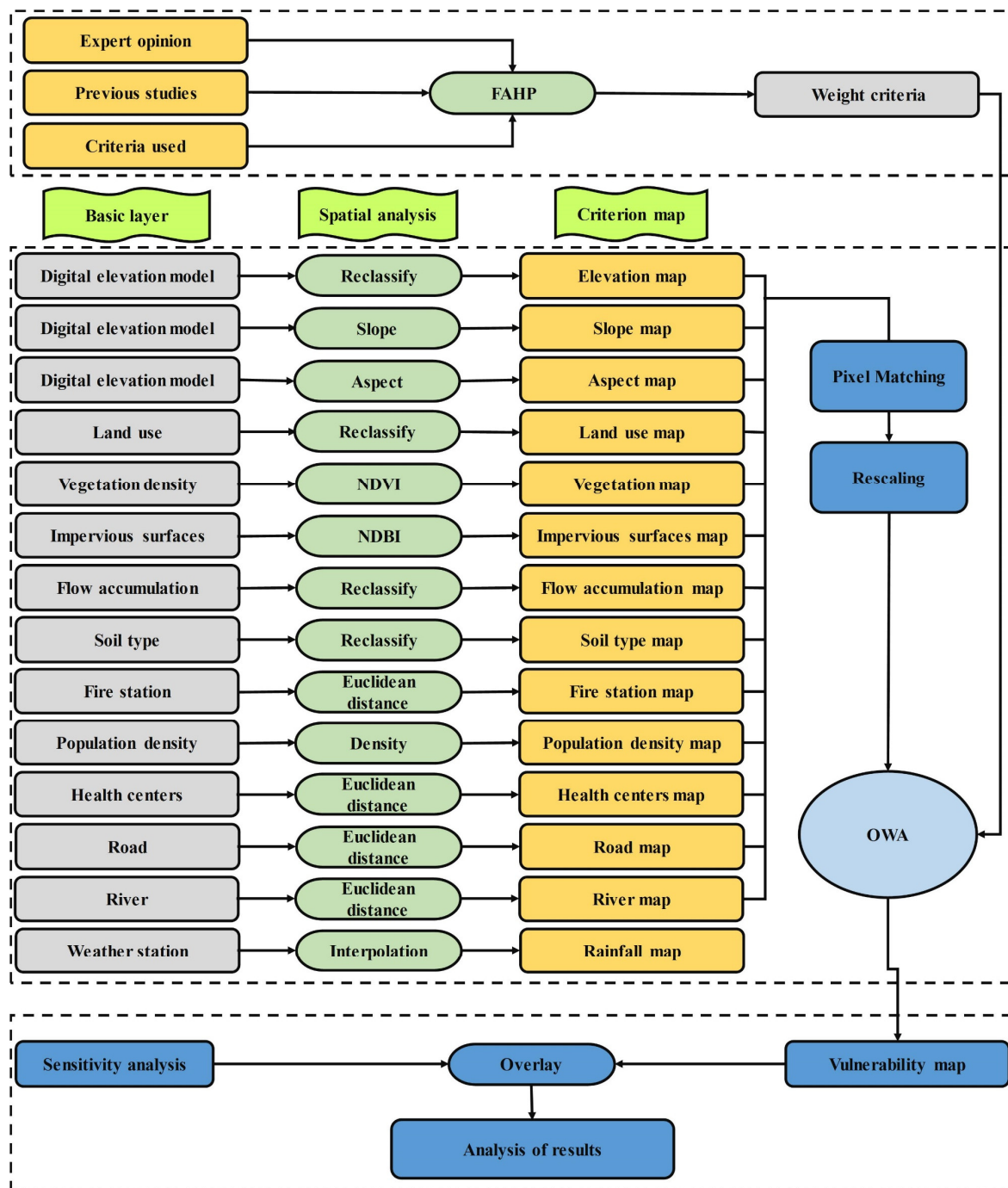
Figure 2. The proposed method for mapping flood vulnerability. Note: Normalized difference vegetation index (NDVI) and Normalized Difference Built-up Index (NDBI).

2.2.1. Rescaling Criteria

After selecting a set of effective criteria to prepare the vulnerability map, each criterion was stored as a GIS map in a spatial database. Depending on the type of criteria, different tools were used to prepare the criteria maps. As an example, the spatial tool "Euclidean distance" was used to prepare a criterion map of "distance from medical centres". To evaluate all the criteria together, it is necessary to convert the layers into comparable units [14,40,41]. The "maximum" values for some criteria and "minimum" values for others are more

important when preparing a vulnerability map, and so the "maximum" and "minimum" values were rescaled. The criteria were divided into two categories: benefit criteria (criteria whose maximum amount is important) and cost criteria (criteria whose minimum amount is important). Benefit criteria included flow accumulation, elevation, slope, aspect, impervious surfaces, population density, and rainfall that have been standardized using Equation (1), and cost criteria included vegetation density, land use, river, health centres, fire station, and soil type standardized using Equation (2) [14].

$$n_{ij} = \frac{r_{ij} - r_{min}}{r_{max} - r_{min}} \tag{1}$$

$$n_{ij} = \frac{r_{max} - r_{ij}}{r_{max} - r_{min}} \tag{2}$$

2.2.2. FAHP

The AHP method is widely used in selecting an option from among other options. However, in this method, pairwise comparisons are made for each level to select the best option using a nine-point scale [42]. Thus, the use of AHP has its weak points: (1) AHP is mainly used in crisp decisions, (2) it examines a very unbalanced scale of judgment (3), uncertainties in individual judgments are not taken into account, and (4) the rating of this method is almost inaccurate [43]. Subjective judgment, choices, and the actions of decision-makers have a huge effect on AHP outcomes. In addition, it is plausible that people's assessments of quality indicators are always subjective and, therefore, inaccurate. Conventional and classical AHP seems inadequate and inefficient in meeting the exact needs of decision-makers. FAHP was proposed in Chang [44] to model this type of uncertainty in human preferences. This combined decision-making technique provides a more accurate understanding of the decision-making process.

The steps for performing Chang's FAHP include the following [44]:

Step 1: Drawing of a hierarchical tree. At this stage, the hierarchical structure of the decision is first drawn using the target, criteria, and sub-criteria levels.

Step 2: Formation of pairwise comparison tables and accountability based on triangular fuzzy numbers in Table 3. In this step, like the AHP method, pairwise comparisons must be created and answered in pairs based on fuzzy numbers.

Table 3. Linguistic scales to express the degree of importance in FAHP.

Fuzzy Numbers	Verbal Expression
(1, 1, 1)	Equal importance
(1, 1.5, 1.5)	Low to moderate preference
(1, 2, 2)	Moderate preference
(3, 3.5, 4)	Moderate to high preference
(3, 4, 4.5)	High preference
(3, 4.5, 5)	High to very high preference
(5, 5.5, 6)	Very high preference
(5, 6, 7)	Very high to quite high preference
(5, 7, 9)	Quite high preference

Step 3: Matrix of pairwise comparisons. At this stage, the agreement matrices are formed according to the decision tree and using the opinions of experts, and then the

compatibility rate is calculated according to the Gogus and Butcher [45] method. The pairwise comparison matrix is calculated from Equation (3):

$$\widetilde{A} = \begin{pmatrix} 1 & \widetilde{a12} & \ldots & \widetilde{a1n} \\ \widetilde{a21} & 1 & \ldots & \widetilde{a2n} \\ \ldots & \ldots & 1 & \ldots \\ \widetilde{an1} & \widetilde{an2} & \ldots & 1 \end{pmatrix} \tag{3}$$

Step 4: Calculation of S_i. The S_i for each row of the pairwise comparison matrix, which is itself a triangular fuzzy number, is calculated from Equation (4):

$$S_i = \sum_{j=1}^{m} M_{g_i}^j \otimes \left[\sum_{i=1}^{n} \sum_{j=1}^{m} M_{g_i}^j \right]^{-1} \tag{4}$$

In this relation, i represents the row number and j represents the column number. $M_{g_i}^j$ in this relation, triangular fuzzy numbers are even comparison matrices. The values of $\sum_{j=1}^{m} M_{g_i}^j$, $\sum_{i=1}^{n} \sum_{j=1}^{m} M_{g_i}^j$, $\left[\sum_{i=1}^{n} \sum_{j=1}^{m} M_{g_i}^j \right]^{-1}$ can be calculated from Equations (5)–(7), respectively:

$$\sum_{j=1}^{m} M_{g_i}^j = \left(\sum_{j=1}^{m} l_j, \sum_{j=1}^{m} m_j, \sum_{j=1}^{m} u_j \right) \tag{5}$$

$$\sum_{i=1}^{n} \sum_{j=1}^{m} M_{g_i}^j = \left(\sum_{i=1}^{n} l_i, \sum_{i=1}^{n} m_i, \sum_{i=1}^{n} u_i \right) \tag{6}$$

$$\left[\sum_{i=1}^{n} \sum_{j=1}^{m} M_{g_i}^j \right]^{-1} = \left(\frac{1}{\sum_{i=1}^{n} u_i}, \frac{1}{\sum_{i=1}^{n} m_i}, \frac{1}{\sum_{i=1}^{n} l_i} \right) \tag{7}$$

In the above Equations, l_i, u_i, and m_i are the first to third components of fuzzy numbers, respectively.

Step 5: Calculation of the degree of S_i relative to each other. In general, if $M_1 = (l_1, m_1, u_1)$ and $M_2 = (l_2, m_2, u_2)$ are two triangular fuzzy numbers, according to the pairwise comparison matrix, the magnitude of the ratio M_1 to M_2 is defined as Equation (8):

$$V(M_2 \geq M_1) = \begin{cases} 1 & \text{if} & m_2 \geq m_1 \\ 0 & \text{if} & l_1 \geq u_2 \\ \frac{l_1 - u_2}{(m_2 - u_2) - (m_1 - l_1)} & & \text{otherwise} \end{cases} \tag{8}$$

On the other hand, the magnitude of a triangular fuzzy number is obtained from K of another triangular fuzzy number from Equation (9):

$$V(M \geq M_1, M_2, \ldots, M_k) = V(V \geq M_1) \text{ and } (M \geq M_2) \text{and} \ldots \text{and } (M \geq M_k) = \min V(M \geq M_I), \; i = 1, 2, \ldots, k \tag{9}$$

Step 6: Calculation of the weight of criteria and alternatives. Equation (10) is used to obtain the weights of criteria and alternatives in pairwise comparison matrices:

$$d'(A_i) = \text{Min } V \, (S_i \geq S_k) \text{ for } k = 1, 2, \ldots, n; \; k \neq i \tag{10}$$

Therefore, the non-normalized weight vector will be in Equation (11):

$$W\prime = \left(d'^{(A_1)}, d'^{(A_2)} \ldots d'^{(A_n)} \right) \text{ Where } A(i = 1, 2, \ldots n) \tag{11}$$

Step 7: Calculation of the final weight vector. To calculate the final weight vector, the weight vector calculated in the previous step must be normalized, using Equation (12):

$$W = (d(A_1, d(A_2), \ldots, d(A_n))^T \tag{12}$$

2.2.3. OWA Operator

In multi-criteria decision making (MCDM), the goal is to integrate the criteria with a general decision function. The weighted average weighting method introduced by Yager [46], which uses aggregation operators, introduces the general decision function. This is a method of combining criteria in multi-criteria decision-making by establishing Equation (13) for a set of input data $x = (x_1 x_2 \ldots x_n)$ that are to be aggregated:

$$F_v = (x_1. \ldots x_n) \sum_{i=1}^{n} v_i \, b_i. \, x \in I^n \tag{13}$$

where b_i, the ith value of x, is sorted from ascending to descending weights, and v_i is the element vector OWA operator's degree. The OWA operator consists of two characteristics that indicate the behavior of the OWA operator: (i) degree of ORness or risk-taking, and (ii) the trade-off between criteria [47,48].

The degree of ORness or risk-taking indicates the position of the OWA operator between the AND (minimum) and OR (maximum) relationships. This degree indicates the degree to which the decision-maker emphasizes the worse or better values of a set of criteria or the risk-aversion and risk-taking of the decision-maker [49]. The degree of ORness is defined using the following Equation (14):

$$\text{ORness} = \frac{1}{n-1} \sum_{i=1}^{n} (n - i) v_i, \qquad 0 \leq \text{ORness} \leq 1 \tag{14}$$

The higher the ORness, the more optimistic or risk-taking the decision-maker, and the lower the ORness, the greater the decision-maker's pessimism or risk-aversion [50]. In general, an OWA operator with an ORness greater than 0.5 represents a risk-taking and optimistic decision-maker. An ORness = 0.5 represents a neutral decision-maker, and an Orness less than 0.5 represents a risk-averse and pessimistic decision-maker [51,52]. It should be noted that the closer the behavior of the OWA operator to the OR or MAX operators, the closer the Orness value is to 1. While the behavior of this operator is closer to the AND and MIN operators, the Orness value is closer to 0. Therefore, the vectors $V_* = (0.0.0. \ldots .1)^T$ as the weight vector of the AND operator and $V^* = (1.0 \ldots .0)^T$ as the OR operator, and $V_A = \left(\frac{1}{n}. \frac{1}{n} \ldots . \frac{1}{n} \right)$ as the weight vector of the weighted linear combination (WLC) operator, are shown in Equation (15):

$$\text{ORness} (V_*) = 0. \text{ ORness} (V^*) = 1. \text{ ORness} (V_A) = 0.5 \tag{15}$$

The second characteristic of the OWA operator is the degree of trade-off between the criteria. The degree of trade-off indicates the extent to which one criterion is exchanged or affected by other criteria [53]. The trade-off is defined as Equation (16):

$$\text{trade} - \text{off} = 1 - \sqrt{\frac{n}{n-1} \sum_{i=1}^{n} (V_i - \frac{n}{n-1})^2}. \, 0 \leq \text{trade} - \text{off} \leq 1 \tag{16}$$

According to the two main characteristics of the OWA operator, a wide range of different risk conditions can be defined, and a vulnerability map can be generated for each

condition. Different scenarios are placed in the triangular space shown in Figure 3. This triangle, in other words, represents the decision space of the OWA operator.
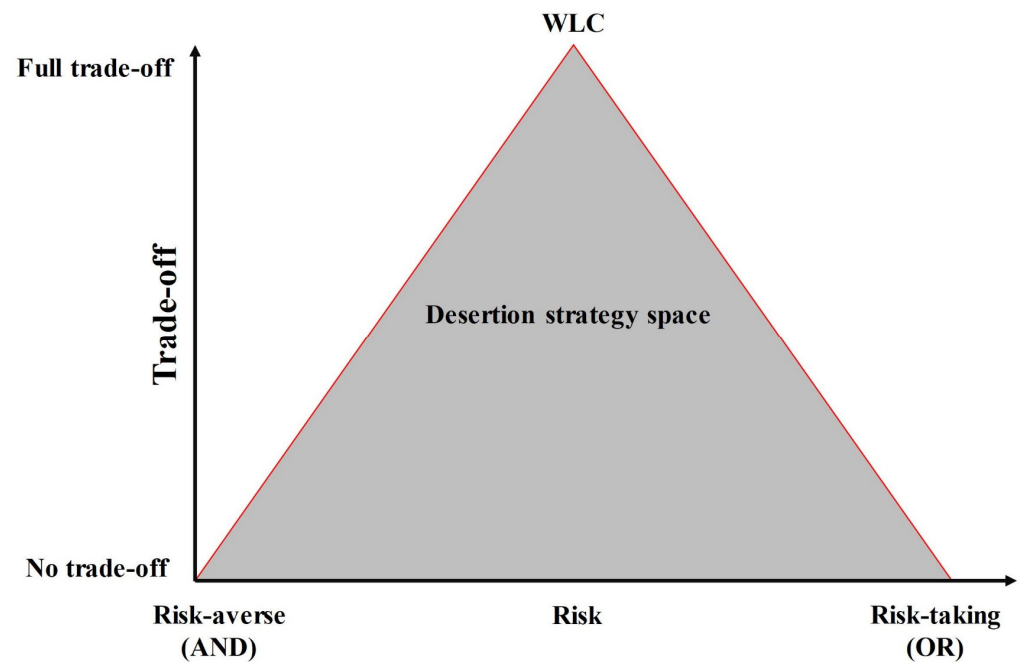

Figure 3. Decision strategy space with OWA operator (different risk conditions).

According to Figure 3, it should be said that the minimum risk is the same as the AND operator, the maximum risk is the OR operator, and the average risk is the weighted linear combination (WLC) operator. Naturally, different scenarios of operators can be generated between AND and OR.

2.2.4. Sensitivity Analysis

One of the most important steps in a multi-criteria evaluation analysis is the sensitivity analysis. Sensitivity analysis is generally the study of the effectiveness of the output results of the input variables of a model [54]. Obviously, due to the existence of different sources of errors, the final output of the evaluation models, which is the ranking of options, is also affected by these errors, and the accuracy of the results should be checked [55,56]. In multi-criteria evaluation, sensitivity analysis is performed with systematic changes in the weight and values of the criteria, and its effect on the final ranking of options is performed [57]. In other words, by analyzing the sensitivity of a multi-criteria evaluation model, the variability in the final results of the model (consistency of results) is investigated [58]. Given that the weight of the criteria is obtained using expert opinions that are accompanied by subjective judgments, the probability of error within them is higher, so if applying changes in the weight of the criteria and re-evaluating the final results of the evaluation of changes was not significant, the results of the model can be trusted [59]. A common method of sensitivity analysis is to increase or decrease the weight of a criterion by P percent, so that the sum of the new weights is equal to one, as in Equation (17). The weight of the other criteria (Ci) is also reduced or increased by the ratio given in Equation (18) [60]:

$$W(P) = \sum_{1}^{n} W\,(C_i,\,P) = 1 \tag{17}$$

where $W\,(C_i,\,P)$ is the i-th standard weight in changes of P percent. If the mth criterion changes by P as a percentage, its new value is obtained from Equation (18):

$$W(C_m, P) = W(C_m, 0) + W(C_m, 0) \times P,\ 1 \le m \le n \tag{18}$$

In addition, the weight of other criteria for establishing in Equation (17) is obtained from Equation (19):

$$W(C_i, P) = (1 - W(C_m, P)) \times W(C_i, 0)/(1 - W(C_m, 0)), \; i \neq m, \; 1 \leq i \leq n \qquad (19)$$

3. Results

The weight of each of the criteria used was determined according to the opinions of 33 experts (including specialists in urban management, GIS, and flood engineering) and the FAHP method (Figure 4). Criterion weight values are between 0 and 1, with the former indicating the least importance and the latter indicating high importance. The sum of the values of all criteria is 1. Among the criteria selected to prepare the flood vulnerability map, the criteria of population density and soil type had the highest and lowest weight and importance, respectively. According to the results, the adjustment rate for calculating the weight of the criteria based on expert opinions is less than 0.1. In other words, it shows the acceptability and compatibility of experts' opinions.
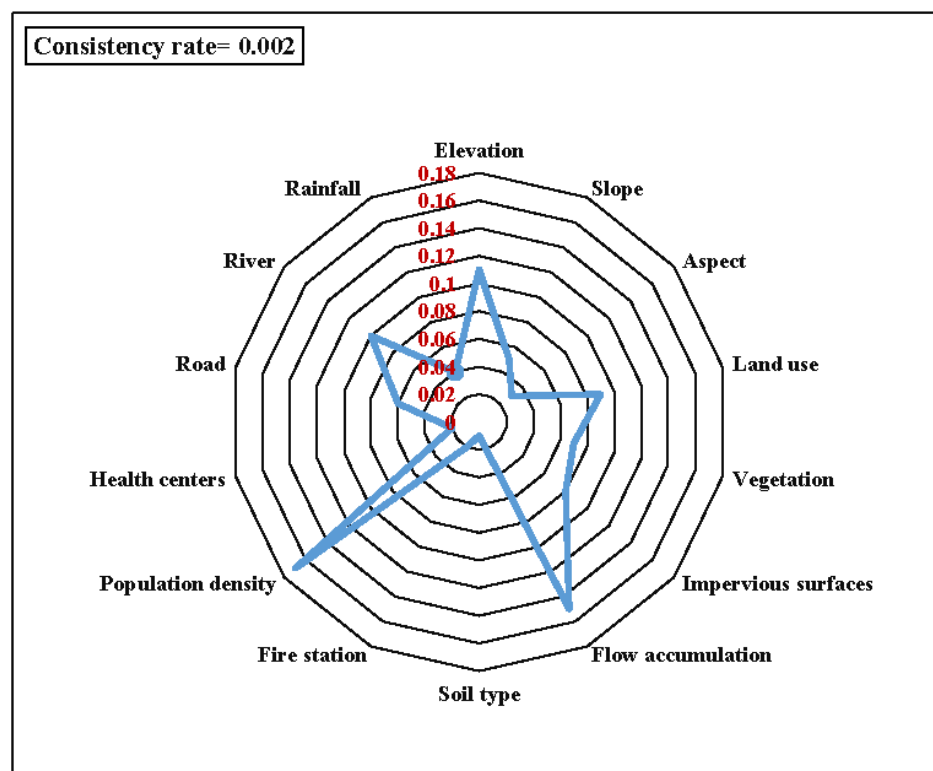

Figure 4. Weight and importance of criteria affecting flood vulnerability.

For each criterion, a map of different criteria was prepared using spatial analysis (Figure 5). For example, using "Euclidean Distance" and "Interpolation" spatial analyses, distance from river and rainfall maps were prepared, respectively. The values of the criteria are normalized between 0 and 1 using the minimum and maximum methods, with a value of 0 indicating a very low vulnerability and 1 indicating a very high vulnerability. Areas with high vulnerability are different in each criterion. This feature of the criteria indicates that each area has a specific vulnerability. Finally, areas that have the highest values in all criteria and thus very high vulnerabilities are selected. For example, in the criteria map of elevation and slope, the northern and northeastern regions have a high elevation and slopes because they are close to the Alborz mountain range, which indicates that these regions are more vulnerable than other regions. In addition, the standard population density map shows that the central regions have a high density due to the density of service and commercial activities, which makes them more vulnerable than other regions.
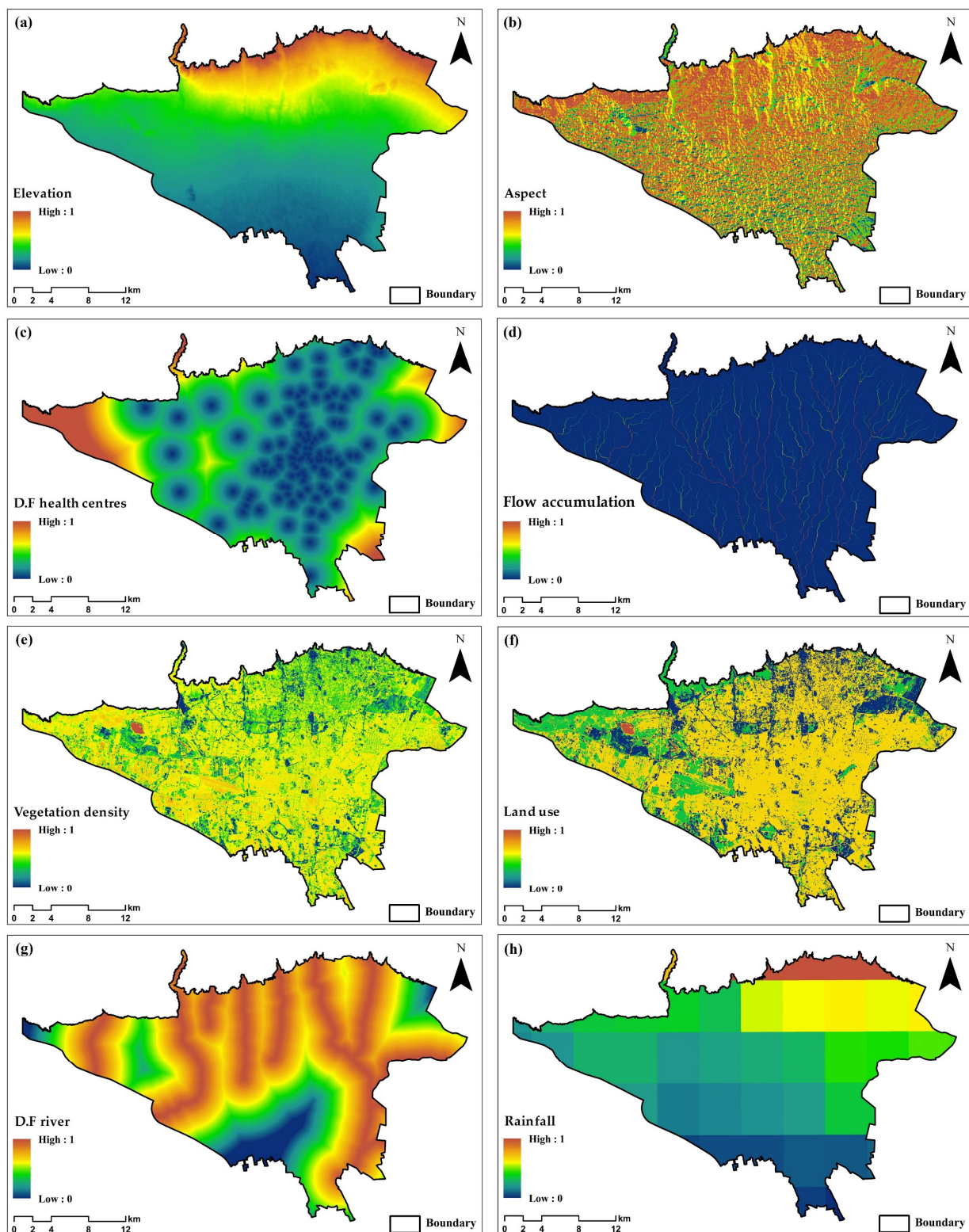
Figure 5. *Cont.*
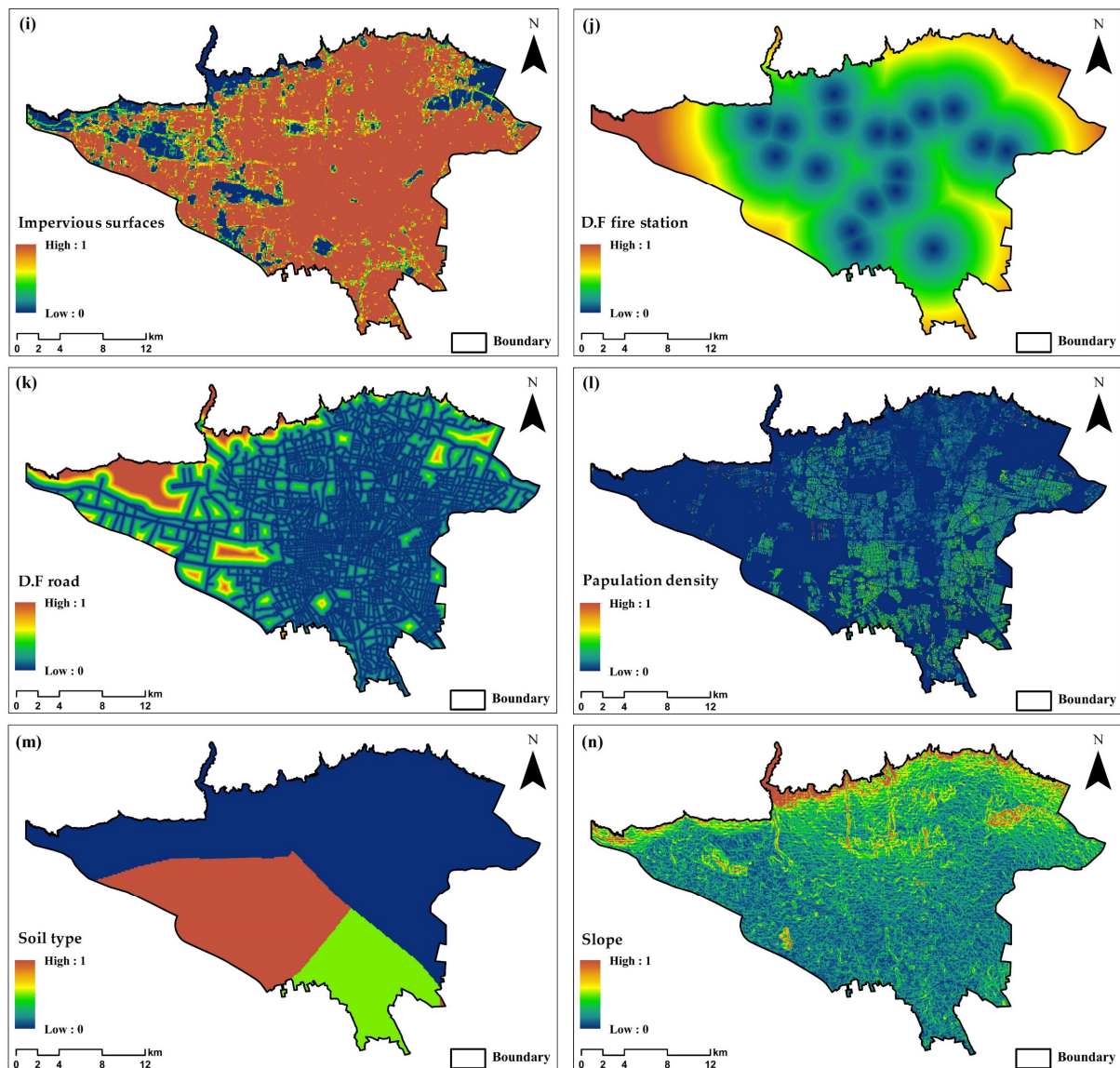
Figure 5. The criteria map (**a**) elevation; (**b**) aspect; (**c**) distance from health centres; (**d**) flow accumulation; (**e**) vegetation density; (**f**) land use; (**g**) distance from river; (**h**) rainfall; (**i**) impervious surfaces; (**j**) distance from fire station; (**k**) distance from road; (**l**) papulation density; (**m**) soil type; (**n**) slope.

Vulnerability maps can be generated in different risk scenarios (from the most pessimistic to the most optimistic) through the equations provided in the previous sections. Vulnerability maps in this study have been generated for 11 different risk scenarios (ORness = 0, 0.1, 0.2, . . . , 1) (Figure 6). In these maps, the degree of vulnerability of each pixel is shown with a real number in the range [0,1], and finally, the pixels are classified into five vulnerability classes: "very low" (0–0.2), "low" (0.2–0.4), "moderate" (0.4–0.6), "high" (0.6–0.8), and "very high" (0.8–1).
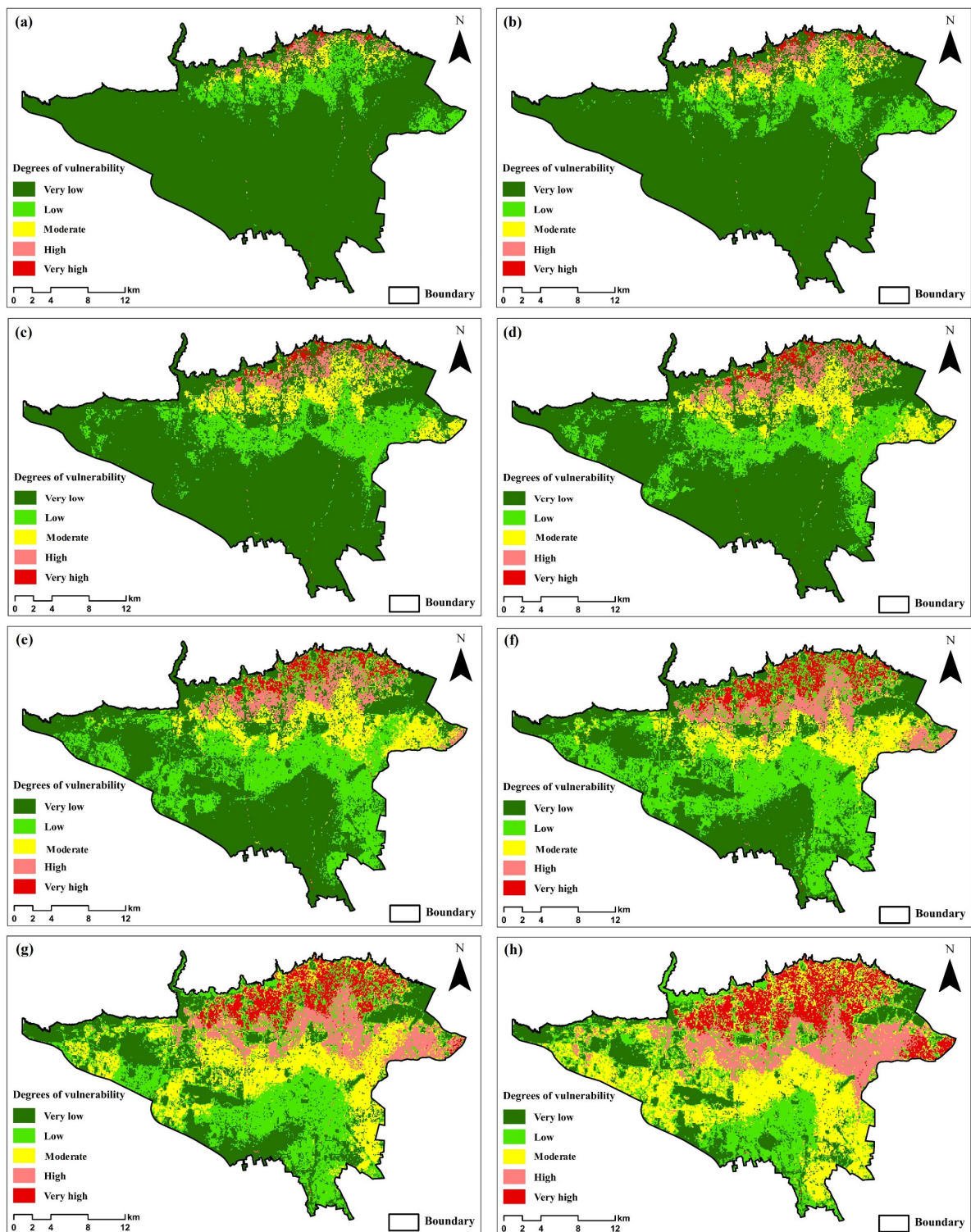
Figure 6. *Cont.*
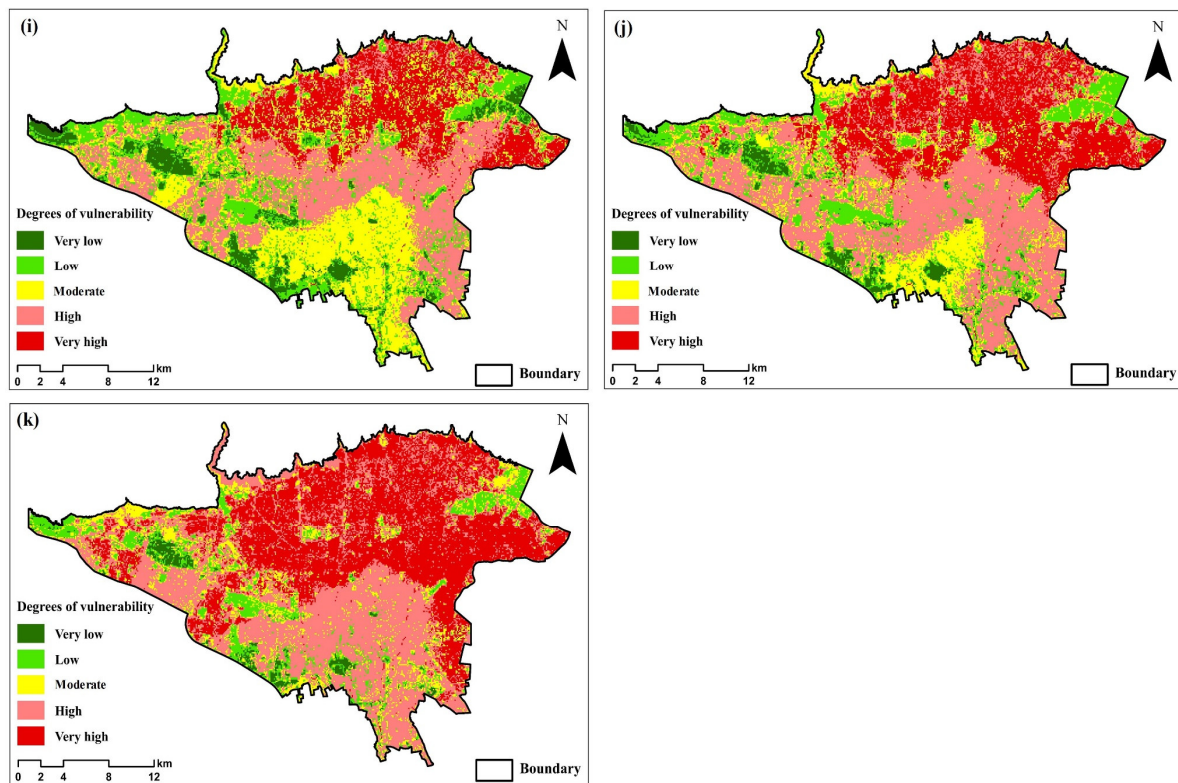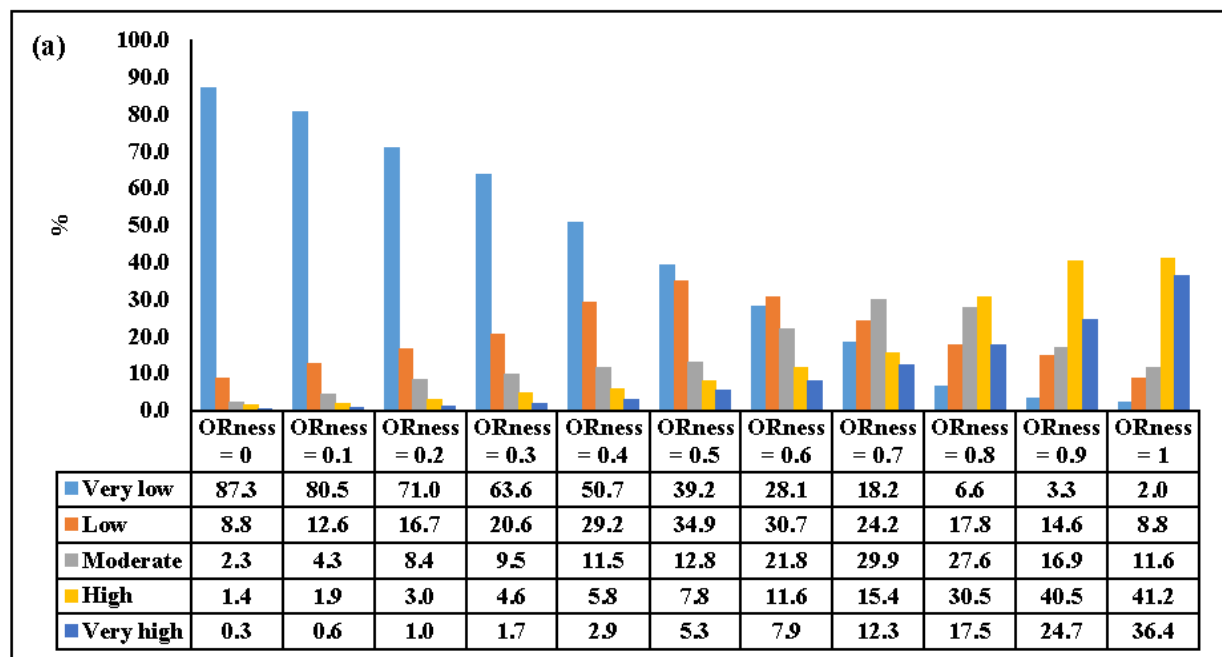
Figure 6. Flood vulnerability map (**a**) ORness = 0; (**b**) ORness = 0.1; (**c**) ORness = 0.2; (**d**) ORness = 0.3; (**e**) ORness = 0.4; (**f**) ORness = 0.5; (**g**) ORness = 0.6; (**h**) ORness = 0.7; (**i**) ORness = 0.8; (**j**) ORness = 0.9; (**k**) ORness = 1.

Analysis of the results (Table 4) shows that the degree of flood vulnerability increases with an increasing degree of risk-taking. The degree of risk-taking is the proximity of the OWA operator to the OR operator. As the degree of risk-taking increases, the number of pixels in the "very low" vulnerability class decreases, and the number of pixels in the "very high" vulnerability class increases. In other words, in the "very risk-averse" scenario (ORness = 0), the class area with very high vulnerability is 168 hectares, and in the "very risk-taking" scenario (ORness = 1), the class area with very high vulnerability is 22,250 hectares. In the first case (risk-averse), areas are considered vulnerable when all their pixels in all criteria have high values and comprehensiveness. Risk-averse managers and planners in the field of planning and projects related to flood vulnerability reduction mostly seek areas in which all the criteria are effective in the best possible way for the allocation of credit. However, in the second case (risk-taking), the pixels that are most likely to be vulnerable are selected as vulnerable areas. This mode can be used when managers and planners do not have economic and time constraints.

In this study, sensitivity analysis was performed 154 times with a weight change (11 times for each criterion) for all criteria (14 criteria), and vulnerability maps were produced with new weights. The greatest changes compared to the initial state (Figure 7a) were in the sensitivity analysis of the "distance from river" criterion and the least changes were in the sensitivity analysis of the "rainfall" criterion. Considering that by changing the weight of the input criteria, there were no significant changes in the model results, it can be said that, based on the sensitivity analysis test, the results of the model are reliable. As can be seen from Figure 7b, most changes were made at ORness = 0.6, which is negligible. Most changes were about 1% and 5% at most. The results of weight change were much less for other criteria, which indicates the acceptable stability of the results of the vulnerability model in different scenarios of sensitivity analysis, i.e., high reliability of the model results.

Table 4. Areal coverage of different vulnerability scenarios across different ORness (ha).

	Very Low	Low	Moderate	High	Very High
ORness = 0	53,318	5366	1411	846	168
ORness = 0.1	49,221	7697	2639	1178	374
ORness = 0.2	43,359	10,205	5121	1806	618
ORness = 0.3	38,859	12,603	5834	2800	1013
ORness = 0.4	30,958	17,821	7019	3515	1795
ORness = 0.5	23,957	21,301	7808	4779	3263
ORness = 0.6	17,145	18,774	13,302	7091	4797
ORness = 0.7	11,104	14,798	18,256	9405	7545
ORness = 0.8	4017	10,865	16,884	18,628	10,714
ORness = 0.9	2003	8931	10,348	24,756	15,071
ORness = 1	1220	5360	7103	25,176	22,250

Figure 7. *Cont.*

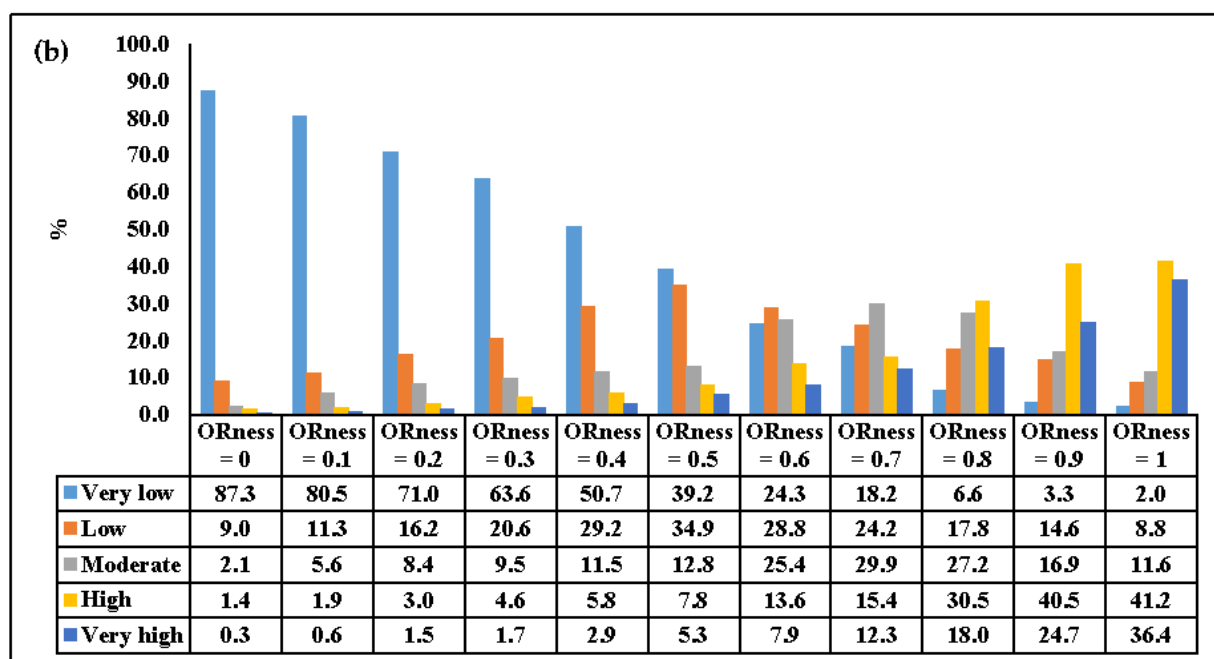|	ORness = 0	ORness = 0.1	ORness = 0.2	ORness = 0.3	ORness = 0.4	ORness = 0.5	ORness = 0.6	ORness = 0.7	ORness = 0.8	ORness = 0.9	ORness = 1
Very low	87.3	80.5	71.0	63.6	50.7	39.2	24.3	18.2	6.6	3.3	2.0
Low	9.0	11.3	16.2	20.6	29.2	34.9	28.8	24.2	17.8	14.6	8.8
Moderate	2.1	5.6	8.4	9.5	11.5	12.8	25.4	29.9	27.2	16.9	11.6
High	1.4	1.9	3.0	4.6	5.8	7.8	13.6	15.4	30.5	40.5	41.2
Very high	0.3	0.6	1.5	1.7	2.9	5.3	7.9	12.3	18.0	24.7	36.4

Figure 7. (**a**) Vulnerability sensitivity analysis with initial weights; (**b**) vulnerability sensitivity analysis by changing the weight criterion of the distance from river.

4. Discussions

Iran has been witnessing a large number of natural hazards, in particular floods, due to the massive mountainous basins in the country as well as the long drought seasons that turn flash floods to devastating events. Tehran has been affected by a large number of floods and carries a large risk of citizens, infrastructure, and assets to them. Hence, this study aimed at proposing a spatial decision support system for identifying vulnerable areas using the GIS-MCDA combination to inform the decision makers and stakeholders about the potential flood damages so that they can build resilience against them.

The preparation of a flood vulnerability mapping at different risk levels used in this study consists of two major steps. In the first step, using the research background and the expert knowledge, the effective influential criteria for floods were identified. In the second step, a flood vulnerability map was prepared for different risk scenarios. Based on our knowledge of past studies and expert opinion, a comprehensive set of criteria including topographical and hydrological characteristics, demographics, vegetation, land use, and urban features was included in the flood vulnerability assessment. The FAHP method was used to determine the weight of the criteria. Most previous articles have used the AHP model. However, this approach is criticized in terms of accounting for uncertainty of ranking priorities of the scoring criteria [61,62]. The FAHP model allows decision makers to better define their preferences in fuzzy environments [63]. This model has been used for weighting the criteria for the allocation of landfills [64], solar farms [65], hospitals [66], wind farms [67], and electric vehicle charging stations [67]. In addition, in these studies, different models based on MCDA such as WLC and AHP have been used to combine the criteria. Each of these models has advantages and disadvantages. One of the most important limitations of these models is lack of considering the concept of risk in decision making. Therefore, in this study, the OWA model was used to map the flood vulnerability. OWA outputs flood vulnerability maps for various risk-based decision scenarios. In recent years, the efficiency of this model has been confirmed in a number of studies for the allocation of renewable energy farms [50] and residential complexes [68], tourism planning [69], thermal comfort mapping [70], and placing municipal solid waste landfills [71]. Our sensitivity analysis showed that the change in the weight of the criteria did not lead to large changes in the areal extent of the vulnerability classes, which is an

advantage. Furthermore, due to the flexibility of our approach in terms of data type and format and there being no dependency on geographical conditions, the proposed approach can be used for other case studies globally.

5. Conclusions and Recommendations

Unprecedented population growth, unregulated land governance, e.g., allocation of land around rivers and canals for development and increased soil sealing due to development activities, and lack of innovative nature-based solutions for such practices in developing countries have caused urban floods across the world, jeopardizing human lives and urban infrastructure. Vulnerability mapping to urban floods and identifying high-risk areas can inform stakeholders and urban planners across different stages of the hazard management cycle, i.e., the pre-crisis, during-crisis and post-crisis phases, which can promote societal security in times of crises. This study demonstrated the design and implementation of a methodical approach for vulnerability mapping for an exemplary case study of Tehran with its unique placement in the slope of the high Alborz Mountains. The analysis of the importance of factors using FAHP showed that the variables of population density, flow accumulation and the river's footprint are more important. The results of flood vulnerability mapping showed that the northern and eastern regions are highly susceptible to floods because runoff caused by rainfall in the northern and eastern mountains of Tehran enters the urban area of Tehran by rivers and canals. Our findings proved that the OWA model is very flexible in combining large input factors for vulnerability mapping across diverse risk scenarios for spatial decision-making processes. The different risk scenarios ranges from very pessimistic to very optimistic scenarios in which the degree of optimism in decision-making increases as the percentage of risk increases too. A risk-averse decision-maker accounts for very difficult conditions in decision-making. Therefore, between different options, it chooses an option that has ideal conditions in terms of different criteria, so the number of suitable options in this case is limited. For risk-taking decision-makers, it is the opposite.

Vulnerability maps borne by this study can serve as analytical tools for providing solutions to reduce vulnerability through different practices such as re-allocation of infrastructure, residential and industrial activities exposed to risk, adaptation of nature-based solutions, and landscape engineering for mitigating the impacts of urban floods. Other applications of vulnerability maps include informing land management plans, urban planning, land-use allocation, land-use change, and per capita land use determination.

As per the research outlook, we recommend (a) to model urban morphological vulnerability, including the network of roads and facilities; (b) to include the future urban development plans in the analysis and potential urban and population growth; (c) to account for climate change impacts for such analysis such as futuristic projection of rainfall; (d) to assess the social, economic, and environmental vulnerabilities caused by floods; e) to elaborate the inclusion of expert knowledge and stakeholder analysis by opening up the discussion table to them ensuring co-designing the methodical approach alongside them; (f) development of a flood warning system available to the public for real-time awareness of flood hazards that can contribute to societal security in the urban environments; (g) to account for uncertainty for such studies and inform the end-users about the uncertainties associated with the achieved results ensuring less bias in the consecutive decisions. The latter can be applied based on fuzzy logic, e.g., type II fuzzy and intuitive fuzzy.

Conflicts of Interest: The authors declare no conflict of interest.

References

1. Yariyan, P.; Avand, M.; Abbaspour, R.A.; Torabi Haghighi, A.; Costache, R.; Ghorbanzadeh, O.; Janizadeh, S.; Blaschke, T. Flood susceptibility mapping using an improved analytic network process with statistical models. *Geomat. Nat. Hazards Risk* **2020**, *11*, 2282–2314. [CrossRef]
2. Ajjur, S.B.; Mogheir, Y.K. Flood hazard mapping using a multi-criteria decision analysis and GIS (case study Gaza Governorate, Palestine). *Arab. J. Geosci.* **2020**, *13*, 44. [CrossRef]
3. Yazdani, M.; Mojtahedi, M.; Loosemore, M.; Sanderson, D. A modelling framework to design an evacuation support system for healthcare infrastructures in response to major flood events. *Prog. Disaster Sci.* **2022**, *13*, 100218. [CrossRef]
4. Avand, M.; Khiavi, A.N.; Khazaei, M.; Tiefenbacher, J.P. Determination of flood probability and prioritization of sub-watersheds: A comparison of game theory to machine learning. *J. Environ. Manag.* **2021**, *295*, 113040. [CrossRef] [PubMed]
5. Ishiwatari, M.; Sasaki, D. Investing in flood protection in Asia: An empirical study focusing on the relationship between investment and damage. *Prog. Disaster Sci.* **2021**, *12*, 100197. [CrossRef]
6. Uddin, K.; Matin, M.A. Potential flood hazard zonation and flood shelter suitability mapping for disaster risk mitigation in Bangladesh using geospatial technology. *Prog. Disaster Sci.* **2021**, *11*, 100185. [CrossRef]
7. Janizadeh, S.; Avand, M.; Jaafari, A.; Phong, T.V.; Bayat, M.; Ahmadisharaf, E.; Prakash, I.; Pham, B.T.; Lee, S. Prediction success of machine learning methods for flash flood susceptibility mapping in the Tafresh watershed, Iran. *Sustainability* **2019**, *11*, 5426. [CrossRef]
8. Talukdar, S.; Ghose, B.; Salam, R.; Mahato, S.; Pham, Q.B.; Linh, N.T.T.; Costache, R.; Avand, M. Flood susceptibility modeling in Teesta River basin, Bangladesh using novel ensembles of bagging algorithms. *Stoch. Environ. Res. Risk Assess.* **2020**, *34*, 2277–2300. [CrossRef]
9. Qin, H.-P.; Li, Z.-X.; Fu, G. The effects of low impact development on urban flooding under different rainfall characteristics. *J. Environ. Manag.* **2013**, *129*, 577–585. [CrossRef]
10. Douglas, I.; Alam, K.; Maghenda, M.; Mcdonnell, Y.; McLean, L.; Campbell, J. Unjust waters: Climate change, flooding and the urban poor in Africa. *Environ. Urban.* **2008**, *20*, 187–205. [CrossRef]
11. Skougaard Kaspersen, P.; Høegh Ravn, N.; Arnbjerg-Nielsen, K.; Madsen, H.; Drews, M. Comparison of the impacts of urban development and climate change on exposing European cities to pluvial flooding. *Hydrol. Earth Syst. Sci.* **2017**, *21*, 4131–4147. [CrossRef]
12. Pandey, A.C.; Kaushik, K.; Parida, B.R. Google Earth Engine for large-scale flood mapping using SAR data and impact assessment on agriculture and population of Ganga-Brahmaputra basin. *Sustainability* **2022**, *14*, 4210. [CrossRef]
13. Luo, T.; Maddocks, A.; Iceland, C.; Ward, P.; Winsemius, H. World's 15 Countries with the Most People Exposed to River Floods. 2015. Available online: https://www.wri.org/insights/worlds-15-countries-most-people-exposed-river-floods (accessed on 5 March 2015).
14. Boloorani, A.D.; Shorabeh, S.N.; Samany, N.N.; Mousivand, A.; Kazemi, Y.; Jaafarzadeh, N.; Zahedi, A.; Rabiei, J. Vulnerability mapping and risk analysis of sand and dust storms in Ahvaz, Iran. *Environ. Pollut.* **2021**, *279*, 116859. [CrossRef] [PubMed]
15. Muris, P.; Schmidt, H.; Lambrichs, R.; Meesters, C. Protective and vulnerability factors of depression in normal adolescents. *Behav. Res. Ther.* **2001**, *39*, 555–565. [CrossRef]
16. Mahmoudzadeh, H.; Mousazadeh, A. Assessing Site Selection of subway routes of the metropolis of Tabriz for natural hazards with an emphasis on flood and earthquake. *J. Nat. Environ. Hazards* **2021**, *9*, 91–110.
17. Moghadas, M.; Asadzadeh, A.; Vafeidis, A.; Fekete, A.; Kötter, T. A multi-criteria approach for assessing urban flood resilience in Tehran, Iran. *Int. J. Disaster Risk Reduct.* **2019**, *35*, 101069. [CrossRef]
18. Rezvani, M.; Nickravesh, F.; Astaneh, A.D.; Kazemi, N. A risk-based decision-making approach for identifying natural-based tourism potential areas. *J. Outdoor Recreat. Tour.* **2022**, *37*, 100485. [CrossRef]
19. Shorabeh, S.N.; Firozjaei, M.K.; Nematollahi, O.; Firozjaei, H.K.; Jelokhani-Niaraki, M. A risk-based multi-criteria spatial decision analysis for solar power plant site selection in different climates: A case study in Iran. *Renew. Energy* **2019**, *143*, 958–973. [CrossRef]
20. Shahpari Sani, D.; Mahmoudian, H. Identifying and Prioritizing Of the Effective Factor on the Tendency of Immigration in Abadan City Using Multi-Criteria Decision Making Techniques. *J. Popul. Assoc. Iran* **2019**, *13*, 89–118.
21. Kaymaz, Ç.K.; Çakır, Ç.; Birinci, S.; Kızılkan, Y. GIS-Fuzzy DEMATEL MCDA model in the evaluation of the areas for ecotourism development: A case study of "Uzundere", Erzurum-Turkey. *Appl. Geogr.* **2021**, *136*, 102577. [CrossRef]
22. Shorabeh, S.N.; Varnaseri, A.; Firozjaei, M.K.; Nickravesh, F.; Samany, N.N. Spatial modeling of areas suitable for public libraries construction by integration of GIS and multi-attribute decision making: Case study Tehran, Iran. *Libr. Inf. Sci. Res.* **2020**, *42*, 101017. [CrossRef]
23. Abdullateef, L.; Tijani, M.N.; Nuru, N.A.; John, S.; Mustapha, A. Assessment of groundwater recharge potential in a typical geological transition zone in Bauchi, NE-Nigeria using remote sensing/GIS and MCDA approaches. *Heliyon* **2021**, *7*, e06762. [CrossRef] [PubMed]

24. Shorabeh, S.N.; Samany, N.N.; Minaei, F.; Firozjaei, H.K.; Homaee, M.; Boloorani, A.D. A decision model based on decision tree and particle swarm optimization algorithms to identify optimal locations for solar power plants construction in Iran. *Renew. Energy* **2022**, *187*, 56–67. [CrossRef]

25. Erbaş, M.; Kabak, M.; Özceylan, E.; Çetinkaya, C. Optimal siting of electric vehicle charging stations: A GIS-based fuzzy Multi-Criteria Decision Analysis. *Energy* **2018**, *163*, 1017–1031. [CrossRef]

26. Mijani, N.; Shahpari Sani, D.; Dastaran, M.; Karimi Firozjaei, H.; Argany, M.; Mahmoudian, H. Spatial modeling of migration using GIS-based multi-criteria decision analysis: A case study of Iran. *Trans. GIS* **2022**, *26*, 645–668. [CrossRef]

27. Atijosan, A.O.; Isa, I.; Abayomi, A. Urban flood vulnerability mapping using integral value ranked fuzzy AHP and GIS. *Int. J. Hydrol. Sci. Technol.* **2021**, *12*, 16–38. [CrossRef]

28. Irawan, A.M.; Marfai, M.A.; Nugraheni, I.R.; Gustono, S.T.; Rejeki, H.A.; Widodo, A.; Mahmudiah, R.R.; Faridatunnisa, M. Comparison between averaged and localised subsidence measurements for coastal floods projection in 2050 Semarang, Indonesia. *Urban Clim.* **2021**, *35*, 100760. [CrossRef]

29. Ku, C.-A. Simulating future land use exposure to extreme floods in metropolitan areas based on an integrated framework. *Urban Clim.* **2021**, *35*, 100738. [CrossRef]

30. Ouma, Y.O.; Tateishi, R. Urban flood vulnerability and risk mapping using integrated multi-parametric AHP and GIS: Methodological overview and case study assessment. *Water* **2014**, *6*, 1515–1545. [CrossRef]

31. Rana, I.A.; Asim, M.; Aslam, A.B.; Jamshed, A. Disaster management cycle and its application for flood risk reduction in urban areas of Pakistan. *Urban Clim.* **2021**, *38*, 100893. [CrossRef]

32. Chakraborty, S.; Mukhopadhyay, S. Assessing flood risk using analytical hierarchy process (AHP) and geographical information system (GIS): Application in Coochbehar district of West Bengal, India. *Nat. Hazards* **2019**, *99*, 247–274. [CrossRef]

33. Eini, M.; Kaboli, H.S.; Rashidian, M.; Hedayat, H. Hazard and vulnerability in urban flood risk mapping: Machine learning techniques and considering the role of urban districts. *Int. J. Disaster Risk Reduct.* **2020**, *50*, 101687. [CrossRef]

34. Feloni, E.; Mousadis, I.; Baltas, E. Flood vulnerability assessment using a GIS-based multi-criteria approach—The case of Attica region. *J. Flood Risk Manag.* **2020**, *13*, e12563. [CrossRef]

35. Hadipour, V.; Vafaie, F.; Deilami, K. Coastal flooding risk assessment using a GIS-based spatial multi-criteria decision analysis approach. *Water* **2020**, *12*, 2379. [CrossRef]

36. Rashetnia, S.; Jahanbani, H. Flood vulnerability assessment using a fuzzy rule-based index in Melbourne, Australia. *Sustain. Water Resour. Manag.* **2021**, *7*, 13. [CrossRef]

37. Hussain, M.; Tayyab, M.; Zhang, J.; Shah, A.A.; Ullah, K.; Mehmood, U.; Al-Shaibah, B. GIS-Based Multi-criteria approach for flood vulnerability assessment and mapping in district Shangla: Khyber Pakhtunkhwa, Pakistan. *Sustainability* **2021**, *13*, 3126. [CrossRef]

38. Nadizadeh Shorabeh, S.; Hamzeh, S. Investigating the Effects of environmental and demographic parameters on the spatial distribution of surface temperature of tehran by combining statistical and mono-window models. *Phys. Geogr. Res. Q.* **2019**, *51*, 263–282.

39. Radmehr, A.; Araghinejad, S. Flood vulnerability analysis by fuzzy spatial multi criteria decision making. *Water Resour. Manag.* **2015**, *29*, 4427–4445. [CrossRef]

40. Qureshi, S.; Shorabeh, S.N.; Samany, N.N.; Minaei, F.; Homaee, M.; Nickravesh, F.; Firozjaei, M.K.; Arsanjani, J.J. A New Integrated Approach for Municipal Landfill Siting Based on Urban Physical Growth Prediction: A Case Study Mashhad Metropolis in Iran. *Remote Sens.* **2021**, *13*, 949. [CrossRef]

41. Shorabeh, S.N.; Argany, M.; Rabiei, J.; Firozjaei, H.K.; Nematollahi, O. Potential assessment of multi-renewable energy farms establishment using spatial multi-criteria decision analysis: A case study and mapping in Iran. *J. Clean. Prod.* **2021**, *295*, 126318. [CrossRef]

42. Saaty, T.L. Decision making—the analytic hierarchy and network processes (AHP/ANP). *J. Syst. Sci. Syst. Eng.* **2004**, *13*, 1–35. [CrossRef]

43. Chen, J.-F.; Hsieh, H.-N.; Do, Q.H. Evaluating teaching performance based on fuzzy AHP and comprehensive evaluation approach. *Appl. Soft Comput.* **2015**, *28*, 100–108. [CrossRef]

44. Chang, D.-Y. Applications of the extent analysis method on fuzzy AHP. *Eur. J. Oper. Res.* **1996**, *95*, 649–655. [CrossRef]

45. Gogus, O.; Boucher, T.O. Strong transitivity, rationality and weak monotonicity in fuzzy pairwise comparisons. *Fuzzy Sets Syst.* **1998**, *94*, 133–144. [CrossRef]

46. Yager, R.R. On ordered weighted averaging aggregation operators in multicriteria decisionmaking. *IEEE Trans. Syst. Man Cybern.* **1988**, *18*, 183–190. [CrossRef]

47. Malczewski, J. A GIS-based approach to multiple criteria group decision-making. *Int. J. Geogr. Inf. Syst.* **1996**, *10*, 955–971. [CrossRef]

48. Zabihi, H.; Alizadeh, M.; Kibet Langat, P.; Karami, M.; Shahabi, H.; Ahmad, A.; Nor Said, M.; Lee, S. GIS Multi-Criteria Analysis by Ordered Weighted Averaging (OWA): Toward an integrated citrus management strategy. *Sustainability* **2019**, *11*, 1009. [CrossRef]

49. Malczewski, J.; Chapman, T.; Flegel, C.; Walters, D.; Shrubsole, D.; Healy, M.A. GIS–multicriteria evaluation with ordered weighted averaging (OWA): Case study of developing watershed management strategies. *Environ. Plan. A* **2003**, *35*, 1769–1784. [CrossRef]

50. Firozjaei, M.K.; Nematollahi, O.; Mijani, N.; Shorabeh, S.N.; Firozjaei, H.K.; Toomanian, A. An integrated GIS-based Ordered Weighted Averaging analysis for solar energy evaluation in Iran: Current conditions and future planning. *Renew. Energy* **2019**, *136*, 1130–1146. [CrossRef]

51. Malczewski, J.; Rinner, C. *Multicriteria Decision Analysis in Geographic Information Science*; Springer: Berlin/Heidelberg, Germany, 2015.

52. Nadizadeh Shorabeh, S.; Neysani Samani, N.; Jelokhani-Niaraki, M.R.J.-N. Determination of optimum areas for the landfill with emphasis on the urban expansion trend based on the combination of the Analytical Hierarchy Process and the Ordered Weighted Averaging model. *J. Nat. Environ.* **2017**, *70*, 949–969.

53. Kiavarz, M.; Jelokhani-Niaraki, M. Geothermal prospectivity mapping using GIS-based Ordered Weighted Averaging approach: A case study in Japan's Akita and Iwate provinces. *Geothermics* **2017**, *70*, 295–304. [CrossRef]

54. Ikonen, T. Comparison of global sensitivity analysis methods–application to fuel behavior modeling. *Nucl. Eng. Des.* **2016**, *297*, 72–80. [CrossRef]

55. Saltelli, A.; Tarantola, S.; Chan, K. A role for sensitivity analysis in presenting the results from MCDA studies to decision makers. *J. Multi Criteria Decis. Anal.* **1999**, *8*, 139–145. [CrossRef]

56. Alemdar, K.D.; Kaya, Ö.; Çodur, M.Y. A GIS and microsimulation-based MCDA approach for evaluation of pedestrian crossings. *Accid. Anal. Prev.* **2020**, *148*, 105771. [CrossRef] [PubMed]

57. Erlacher, C.; Anders, K.-H.; Jankowski, P.; Paulus, G.; Blaschke, T. A framework for cloud-based spatially-explicit uncertainty and sensitivity analysis in spatial multi-criteria models. *ISPRS Int. J. Geo Inf.* **2021**, *10*, 244. [CrossRef]

58. Chen, Y.; Yu, J.; Khan, S. Spatial sensitivity analysis of multi-criteria weights in GIS-based land suitability evaluation. *Environ. Model. Softw.* **2010**, *25*, 1582–1591. [CrossRef]

59. Sadeghi-Niaraki, A.; Varshosaz, M.; Kim, K.; Jung, J.J. Real world representation of a road network for route planning in GIS. *Expert Syst. Appl.* **2011**, *38*, 11999–12008. [CrossRef]

60. Eldrandaly, K.A. Exploring multi-criteria decision strategies in GIS with linguistic quantifiers: An extension of the analytical network process using ordered weighted averaging operators. *Int. J. Geogr. Inf. Sci.* **2013**, *27*, 2455–2482. [CrossRef]

61. Vinogradova-Zinkevič, I.; Podvezko, V.; Zavadskas, E.K. Comparative Assessment of the Stability of AHP and FAHP Methods. *Symmetry* **2021**, *13*, 479. [CrossRef]

62. Khashei-Siuki, A.; Sharifan, H. Comparison of AHP and FAHP methods in determining suitable areas for drinking water harvesting in Birjand aquifer. Iran. *Groundw. Sustain. Dev.* **2020**, *10*, 100328. [CrossRef]

63. Hu, J.; Chen, J.; Chen, Z.; Cao, J.; Wang, Q.; Zhao, L.; Zhang, H.; Xu, B.; Chen, G. Risk assessment of seismic hazards in hydraulic fracturing areas based on fuzzy comprehensive evaluation and AHP method (FAHP): A case analysis of Shangluo area in Yibin City, Sichuan Province, China. *J. Pet. Sci. Eng.* **2018**, *170*, 797–812. [CrossRef]

64. Fard, M.B.; Hamidi, D.; Ebadi, M.; Alavi, J.; Mckay, G. Optimum landfill site selection by a hybrid multi-criteria and multi-Agent decision-making method in a temperate and humid climate: BWM-GIS-FAHP-GT. *Sustain. Cities Soc.* **2022**, *79*, 103641. [CrossRef]

65. Thanh, N.V.; Lan, N.T.K. Solar Energy Deployment for the Sustainable Future of Vietnam: Hybrid SWOC-FAHP-WASPAS Analysis. *Energies* **2022**, *15*, 2798. [CrossRef]

66. Tripathi, A.K.; Agrawal, S.; Gupta, R.D. Comparison of GIS-based AHP and fuzzy AHP methods for hospital site selection: A case study for Prayagraj City, India. *GeoJournal* **2021**, *86*, 1–22. [CrossRef]

67. Talinli, I.; Topuz, E.; Aydin, E.; Kabakcı, S.B. A Holistic Approach for Wind Farm Site Selection by FAHP. In *Wind Farm Technical Regulations, Potential Estimation and Siting Assessement*; InTech Open: Rijieka, Croatia, 2011; Volume 3, pp. 213–234.

68. Rajabi, M.; Mansourian, A.; Talei, M. A comparing study between AHP, AHP-OWA and Fuzzy AHP-OWA multi-criteria decision making methods for site selection of residential complexes in Tabriz-Iran. *J. Environ. Stud.* **2011**, *37*, 77–92.

69. Eldrandaly, K.A.; AL-Amari, M.A. An expert GIS-based ANP-OWA decision making framework for tourism development site selection. *Int. J. Intell. Syst. Appl.* **2014**, *6*, 1. [CrossRef]

70. Mijani, N.; Alavipanah, S.K.; Hamzeh, S.; Firozjaei, M.K.; Arsanjani, J.J. Modeling thermal comfort in different condition of mind using satellite images: An Ordered Weighted Averaging approach and a case study. *Ecol. Indic.* **2019**, *104*, 1–12. [CrossRef]

71. Gorsevski, P.V.; Donevska, K.R.; Mitrovski, C.D.; Frizado, J.P. Integrating multi-criteria evaluation techniques with geographic information systems for landfill site selection: A case study using ordered weighted average. *Waste Manag.* **2012**, *32*, 287–296. [CrossRef]